



Research article

Docosahexaenoic acid improves cognition and hippocampal pyroptosis in rats with intrauterine growth restriction

Lijia Wan^{a,b}, Xiaori He^{a,c}, Mingfeng He^{a,c}, Yuanqiang Yu^{a,c}, Weiming Jiang^d, Can Liang^{a,c}, Kaiju Luo^{a,c}, Xiaoyun Gong^{a,c}, Yonghui Yang^{a,c}, Qingyi Dong^{a,c}, Pingyang Chen^{a,c,*}

^a Department of Pediatrics, The Second Xiangya Hospital, Central South University, Changsha, Hunan 410011, PR China

^b Department of Child Healthcare, Hunan Provincial Maternal and Child Health Care Hospital, Changsha, Hunan 410011, PR China

^c Laboratory of Neonatal Disease, Institute of Pediatrics, Central South University, Changsha, Hunan 410011, PR China

^d Children's Institute of Three Gorges University, Yichang Central People's Hospital, The First College of Clinical Medical Sciences, China Three Gorges University, Yichang 443003, PR China



ARTICLE INFO

Keywords:

Intrauterine growth restriction
Small for gestational age
Pyroptosis
DHA
Cognitive impairment
Hippocampus

ABSTRACT

Background and Objective: Intrauterine growth restriction (IUGR) is defined as the failure of a fetus to reach its genetic growth potential in utero resulted by maternal, placental, fetal, and genetic factors. Previous studies have reported that IUGR is associated with a high incidence of neurological damage, although the precise causes of such damage remain unclear. We aimed to investigate whether cognitive impairment in rats with IUGR is related to pyroptosis of hippocampal neurons and determine the effect of early intervention with docosahexaenoic acid (DHA). **Methods:** Learning and memory function was assessed using the Morris water maze test. The morphological structure and ultrastructure of the hippocampus was examined via hematoxylin and eosin staining and electron microscopy respectively. The pyroptosis of hippocampal neuron was detected by gasdermin-D (GSDMD) immunofluorescence staining, mRNA and protein expression of nuclear localization leucine-rich-repeat protein 1 (NLRP1), caspase-1, GSDMD, and quantification of inflammatory cytokines interleukin (IL)-1 β and IL-18 in the hippocampus. **Results:** IUGR rats exhibited decreased learning and memory function, morphological structure and ultrastructural changes in hippocampus compared to controls. IUGR rats also exhibited increased hippocampal quantification of GSDMD immunofluorescence staining, increased mRNA and protein expression of NLRP1, caspase-1, and GSDMD, and increased quantification of IL-1 β and IL-18 in the hippocampus. Intervention with DHA attenuated these effects. **Conclusion:** Cognitive impairment in rats with IUGR may be related to pyroptosis of hippocampal neurons. Early intervention with DHA may attenuate cognitive impairment and reduce hippocampal pyroptosis in rats with IUGR.

* Corresponding author. NO.139, Renmin Middle Road, furong District, Changsha, Hunan 410011, PR China.

E-mail addresses: [wanljia0225@163.com](mailto:wanjia0225@163.com) (L. Wan), hexiaori@csu.edu.cn (X. He), mingfenghe@distinctclinic.com (M. He), yuyuanqiang@csu.edu.cn (Y. Yu), master_jwm@163.com (W. Jiang), liang11can@163.com (C. Liang), luokj200701@163.com (K. Luo), gongxiaoyunhelen@sina.com (X. Gong), yangyonghui@csu.edu.cn (Y. Yang), dongqingyi@csu.edu.cn (Q. Dong), chenpingyang@csu.edu.cn (P. Chen).

<https://doi.org/10.1016/j.heliyon.2023.e12920>

Received 15 September 2022; Received in revised form 4 January 2023; Accepted 9 January 2023

Available online 27 January 2023

2405-8440/© 2023 The Authors. Published by Elsevier Ltd. This is an open access article under the CC BY-NC-ND license (<http://creativecommons.org/licenses/by-nc-nd/4.0/>).

1. Introduction

Intrauterine growth restriction (IUGR) is defined as the failure of the fetus to reach the ideal genetic potential due to maternal, placental and fetal causes, often leading to a birth weight considered small for gestational age (SGA), which is defined as a birth weight more than two standard deviations below the mean weight or below the 10th percentile for neonates of the same gestational age [1].

IUGR is associated with a high incidence of neurological damage, with neurological sequelae such as cognitive impairment occurring in 25–34% of affected children [2,3]. However, the causes of such impairment remain to be fully understood. Numerous studies have demonstrated that neuroinflammation and decreases in hippocampal neurons are two important mechanisms underlying cognitive impairment following IUGR [4–6]. Although additional research indicates that decreases in neuronal number in the hippocampus with low protein diet-induced IUGR are related to apoptosis [7], whether they are related to pyroptosis remains to be determined. Previous studies have demonstrated that pyroptosis is related to cognitive impairment in various diseases, such as post-stroke, vascular dementia and sepsis-associated encephalopathy etc [8–10], however, whether it is related to cognitive impairment in IUGR remains to be clarified.

Pyroptosis is a type of programmed cell death accompanied by an inflammatory response, occurring more quickly than apoptosis, and plays an important role in neurodevelopment [11]. Like apoptosis, pyroptosis induces karyopyknosis and DNA fragmentation; however, the process is not associated with the formation of apoptotic bodies but with formation of plasma membrane pore mediated by gasdermin proteins and the release of cellular contents and proinflammatory cytokines. Thus, pyroptosis is performed by gasdermin proteins and characterized by both apoptosis and necrosis, contributing to neuroinflammation in brain [12].

The activation of pyroptosis can occur in an inflammasome-dependent and -independent manner. And there are canonical and non-canonical pathways in inflammasome-dependent manner. Canonical inflammasome-dependent pyroptosis is mediated by caspase-1 [11]. When the body is exposed to harmful stimuli, intracellular and extracellular danger signals induce the formation of intracytoplasmic inflammasomes via NLRs (NOD-like receptors) bind to pro-caspase-1 through ASC [13]. Following activation by the inflammasome, cleaved caspase-1 promotes the shearing and maturation of the inflammatory cytokines interleukin-1 β (IL-1 β) and interleukin-18 (IL-18) while cleaving gasdermin-D (GSDMD) protein into active GSDMD-N. GSDMD-N insertion into the plasma membrane, forming the plasma membrane pores, leading to increased osmotic pressure, rupture of the plasma membrane, and release of pro-inflammatory factors, ultimately resulting in pyroptosis [14].

Inflammasomes play an important role in pyroptosis and are key regulators of inflammation in health and disease, especially the central nervous system (CNS) diseases. NLRP3 (NOD-like receptor family, pyrin domain containing 3) and NLRP1 (NOD-like receptor family, pyrin domain containing 1) are the most two studied inflammasomes in the CNS. In the CNS, NLRP3 inflammasome is mainly distributed in microglia and NLRP1 inflammasome is mainly distributed in neurons [15]. Docosahexaenoic acid (DHA) is an omega-3 polyunsaturated fatty acids (ω -3 PUFAs) and is the main component of cytomembranes in the brain. In addition to its anti-inflammatory and antioxidant effects, DHA plays an important role in maintaining neuronal plasticity and cognition, thus promoting brain development and improving cognitive function [16,17]. Recent study had revealed that ω -3 PUFAs markedly ameliorated neuronal death and behavioral deficits after traumatic brain injury (TBI), the G protein-coupled receptor 40 (GPR40)-mediated pathway is involved in the inhibitory effects of ω -3 PUFAs on TBI-induced inflammation, and beta-Arrestin-2 (ARRB2) is activated to interact with NLRP3 [18]. However, whether DHA inhibits the activation of NLRP1 inflammasomes has only been confirmed in placental tissue [19] but not in cases of brain injury.

Therefore, in the present study, we aimed to determine whether rats with IUGR exhibit impairments in learning and memory based on performance in the Morris water maze test, following which observed the morphological structure of hippocampus by HE staining, observed the ultrastructure of hippocampal neurons by electron microscopy, examined the quantification and localization of GSDMD by immunofluorescence staining, examined the mRNA and protein expression of NLRP1, caspase-1, GSDMD by quantitative reverse transcription-polymerase chain reaction (RT-qPCR) and western-blot (WB) and examined the quantification of IL-1 β and IL-18 in the hippocampus by ELISA to determine whether these rats exhibit hippocampal neurons pyroptosis. Lastly, we aimed to investigate whether intervention with DHA can attenuate cognitive impairment and hippocampal pyroptosis in rats with IUGR.

2. Materials and methods

2.1. Animals

Animals were treated in accordance with the Guide for the Care and Use of Laboratory Animals and housed in a standardized animal care center at an appropriate temperature and humidity. All animals were housed under a 12-h light/dark cycle and had free access to food and water. All experimental protocols were approved by the Animal Ethics Committee of Central South University (NO. 2019sydw0176).

Three-month-old Sprague–Dawley rats were purchased from the Hunan Slacker Jingda Laboratory Animal Co., Ltd. (Changsha, China) and mated at a ratio of 1:1. Pregnant rats were singly housed and fed either a normal diet with a protein content of 21% or a low-protein diet with a protein content of 10% [7] from the first day of pregnancy until delivery. The offspring of pregnant rats fed with 21% protein diet were identified as normal birth weight (NBW) pups, the offspring of pregnant rats fed with 10% protein diet exhibiting birth weights lower than the 10th percentile of NBW pups were identified as IUGR pups. After giving birth, the mother rats and their offspring rats were housed in a single cage, and all the mothers were fed with normal diet. After 21 days of breastfeeding, the offspring rats were separated from their mothers and fed with normal diet. 40 NBW pups and 40 IUGR pups were randomly selected to participate in the experiment. NBW pups and IUGR pups were randomly divided into the DHA intervention group and control group,

respectively: Group N (NBW), Group ND (NBW + DHA), Group I (IUGR), and Group ID (IUGR + DHA). Based on a normal diet, the DHA intervention group was given a gavage of 300 mg/kg of DHA (30 mg/ml) [20] from days-of-life (DOL) 1 to 28 or 56, while the control group was given a gavage of the same amount of normal saline. Pups in each group were randomly sacrificed via cervical dislocation at DOL 1, 28, and 56, respectively ($n = 8$ for each subgroup), and hippocampal samples were collected for further evaluation. Prior to sacrifice, rats underwent Morris water maze testing to evaluate learning and memory function at DOL 28 and 56 (The experimental protocol see Fig. 1).

2.2. Morris water maze test

The Morris water maze test [21] was designed to test the learning and memory function of rats, conducted 5 days before samples were collected from each group of rats at two-time points: DOL 23–28 and DOL 51–56. The water maze device consisted of a circular pool with a platform hidden under the water, an automatic video recording system, and computer and analysis software. Planlab SMART V3.0 (Harvard Apparatus, USA) was used as the analysis software for water maze in this experiment. The camera connected with the automatic video recording system is suspended above the pool, which can record the rats' swimming paths and video images in the water maze in real time and transmit them to the computer. The circular pool is 80 cm high and 200 cm in diameter, and was divided into four quadrants of the same size. The water in the pool was dyed black with ink. One eye-catching color mark and four different colors were posted in the center of each quadrant wall above the water. A black circular platform with a diameter of 10 cm was placed in the center of the third quadrant and hidden 1.5 cm below the water surface, with its position held constant throughout the experiment. The water temperature was approximately 20 °C. The pool was surrounded by white curtains to make it isolated from the surrounding environment and avoid the interference of sound and light. Choosing the same time period for each experiment, keeping the room light consistent and keeping quiet.

The water maze test program mainly includes place navigation and spatial probe test. (1) The place navigation used to measure the learning ability of rats in the water maze. During the place navigation, the rats were trained four times a day for 5 consecutive days. In each trial, the rats were placed into the pool facing the pool wall from the four-quadrant entry points, and the time required to reach and stand on the hidden platform was recorded as the escape latency (seconds). The trial was limited to a maximum swimming time of 120 s (2) The spatial probe test used to measure the ability of rats to maintain long-term memory. The spatial probe test was conducted on the day after the place navigation. The platform was removed, and the rats were placed into the water from the same entry point in the first quadrant, and Target Crossings were recorded.

2.3. Hematoxylin and eosin (HE) staining

The hippocampi were fixed with 4% paraformaldehyde for at least 24 h before paraffin embedding and cut into sections (thickness: 5 μ m). Slices were baked at 60 °C for 12 h. To deparaffinize the slices to water, the sections were first placed in xylene for 15 min three times each, following which they were placed in 100%, 100%, 95%, 85%, and 75% ethanol successively for 5 min in each grade. The sections were then soaked in distilled water for 5 min, dyed with hematoxylin for 1 min, washed with distilled water, washed with PBS black to blue, dyed with eosin for 30 s, and washed with distilled water. Thereafter, the sections were dehydrated with graded alcohol (95–100%) for 5 min per grade. After removal, the slices were placed in xylene for 10 min twice, sealed with neutral gum, and observed

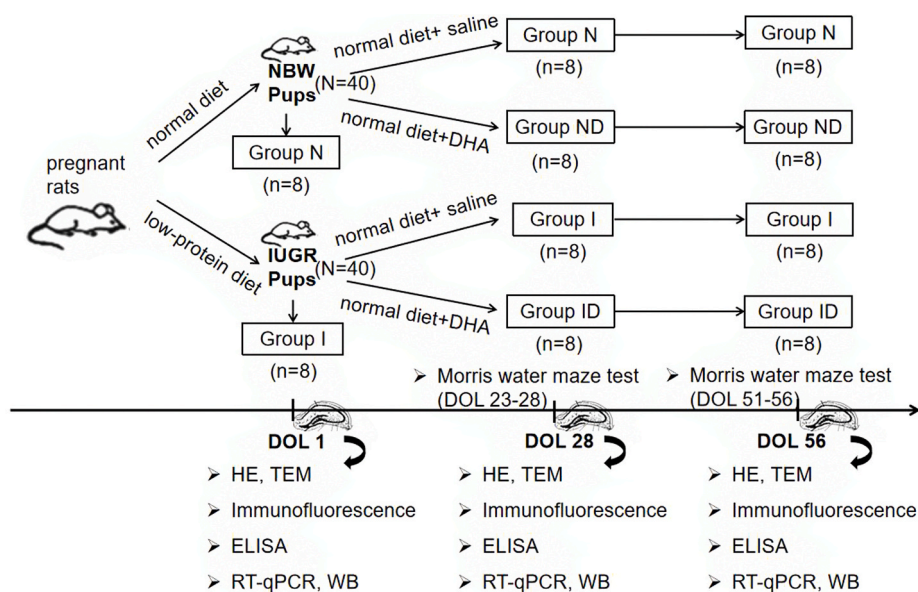


Fig. 1. The experimental protocol.

under a microscope.

2.4. Transmission electron microscopy (TEM) examination

The hippocampi were fixed with 2.5% glutaraldehyde for 6–12 h, bathed with PBS for 1–6 h, and fixed with 1% osmium for 1–2 h. For dehydration, the fixed hippocampi were placed in 30% ethanol for 10 min, 50% ethanol for 10 min, 70% ethanol uranium acetate for 3 h or overnight, 80% ethanol for 10 min, 95% ethanol for 15 min, 100% ethanol for 50 min twice, and epoxy propane for 30 min. For embedding, the tissue was soaked in a 1:1 solution of epoxy propane and epoxy resin for 1–2 h, pure epoxy resin for 2–3 h, and then baked at 40 °C for 12 h and 60 °C for 48 h. The embedded block was then removed, repaired, and cut into ultrathin slices (thickness: 50 nm), which were carefully removed from the bath using a copper net covered by carbon. The ultrathin sections were stained with 4% uranium acetate and lead citrate, following which they were observed via TEM at 80 kV (Hitachi 7700, Japan).

2.5. GSDMD immunofluorescence staining

Heat-Induced Antigen Retrieval of dehydrated sections was done using citrate buffer (0.01 M, pH: 6.0), boiled for 23 min, and cooled for 23 min, following which they were removed and cooled to room temperature. After cooling, the sections were washed with 0.01 M PBS (pH: 7.2–7.6) for 3 min three times each and placed in sodium borohydride solution at room temperature for 30 min. After rinsing in water for 5 min, the sections were placed in Sudan black dye solution at room temperature for 5 min and washed with water for 3 min. They were then placed in 10% normal serum/5% bovine serum albumin (BSA) for 60 min. Then, 5 × Equilibration Buffer was diluted with deionized water at a ratio of 1:5, and 100 µL of the 1 × Equilibration Buffer was added to cover the sample area of each slice for 10–30 min of incubation at room temperature. The slides were washed with PBS for 5 min three times in the dark. Samples were incubated the appropriately diluted primary antibody GSDMD (1:100bs- PA5-30823, Thermo Fisher) overnight at 4 °C, following which they were washed three times with PBS for 5 min each. Then, 50–100 µL of the secondary anti-rabbit immunoglobulin G (IgG)-labeled fluorescent antibody (1:100bs- SA00001-2, Proteintech) was added to the samples, which were incubated at 37 °C for 90 min and washed three times in PBS for 5 min each. The sections were then stained in 4',6-diamidino-2-phenylindole (DAPI) working solution at 37 °C for 10 min and washed three times with PBS for 5 min each. Sections were sealed with buffer glycerin, observed under a scanning fluorescence microscope (Motic BA410T). For each section, 4 fields of view were randomly selected from CA1 area for image acquisition. The nuclei stained by DAPI were blue under UV excitation, and GSDMD positive signal was red fluorescence. Image-Pro Plus 6.0 software (Meyer, USA) was used for quantitative analysis of each Image: positive expression of GSDMD = Integral optical density (IOD) of GSDMD, and the average value of four fields in each section was calculated.

2.6. RT-qPCR analysis the mRNA of NLRP1, caspase-1, and GSDMD

Total RNA was isolated from the hippocampus using a TRIzol kit (15596026, Thermo, USA), while cDNA was synthesized using a reverse transcription kit (CW2569, Kangwei, China). The mRNA levels were quantified via RT-qPCR using an UltraSYBR Mixture (CW2601, Kangwei, China). The PCR primers for NLRP1, caspase-1 and GSDMD are listed in Table 1. The amplification program is listed in Table 2.

2.7. WB analysis the protein of NLRP1, caspase-1, and GSDMD-N

Protein concentrations of NLRP1, caspase-1, and GSDMD-N in the hippocampus were assessed via Western blot analysis. Total proteins were extracted from hippocampal tissues using protein extraction reagents. Following treatment with 10% SDS-PAGE, the proteins were transferred onto a PVDF membrane. The membranes were then incubated with specific primary antibodies at 4 °C overnight, as follows: anti-NLRP1 (1:1000; rabbit, no. ab3683, Abcam), anti-caspase-1 (1:1000; rabbit, ab179515, Abcam), and anti-GSDMD (1:1000; rabbit, PA5-30823, ThermoFisher). The membranes were then incubated with horseradish peroxidase-conjugated secondary antibodies (1:5000; mouse, SA00001-1, Proteintech). β-actin was used as an internal control. Western blot bands were visualized using the ECL Chemiluminescent Substrate and quantified using Quantity One v4.6.6 image analysis software (Bio-Rad, USA).

Table 1
Primers used for RT-qPCR analysis.

Gene	Primer Sequence
NLRP1	F: 5'- AATGATGTGCCCTTAGCCAG-3' R: 5'- CCCTTGGCTTATATGTTACAGACC-3'
Caspase-1	F: 5'- CTAGACTACAGATGCCAACCCAC-3' R: 5'- GGCTTCTTATTGGCAT GAITCCC -3'
GSDMD	F: 5'- TTAGTCTGCTTGCCGTACTCC -3' R: 5'- GTCCTGTAATAATCCTCCCGATG -3'

Table 2
The amplification program for RT-qPCR.

Gene	Temperature	Time
NLRP1/Caspase-1/GSDMD	95 °C	10 min
	95 °C	15 s
	60 °C	30 s
	PCR-HRM : 60°C-95 °C	

2.8. Enzyme-linked immunosorbent assay (ELISA) of IL-1 β and IL-18

The concentration of IL-1 β in the hippocampus was quantified using ELISA kits (KE20005) obtained from Proteintech (Chicago, USA). In contrast, the concentration of IL-18 was quantified using ELISA kits (CSB-E04610r) obtained from Huamei Biological Technology Co. Ltd (Wuhan, China). ELISA was performed in accordance with the manufacturer's instructions. The IOD of each sample was measured at a wavelength of 450 nm using a Molecular Devices system (MB-530, China). The IOD value was taken as the abscissa and the concentration of the standard sample was taken as the ordinate, the standard curve was made using CurveExpert 1.4 software (Hyams, USA). The regression equation of the standard curve was calculated according to the IOD value and the concentration of the standard sample. The IOD value of the target sample was substituted into the equation to calculate the concentration of the target sample.

2.9. Statistical analysis

All statistical analyses were performed using SPSS 23.0 (IBM Corp., Chicago, USA). Data were expressed as the mean \pm standard deviation and were tested for normality. If the data conformed to a normal distribution, comparisons were performed using one-way analyses of variance (ANOVA) (repeated-measures analyses of variance was used in navigation experiment) followed by the least significant difference (LSD) test for pairwise comparison between groups when the variance was uniform, Tamhane test when the variance was uneven. χ^2 test was used to compare the rates between groups. If the data did not conform to a normal distribution, non parametric analyses Friedman were used. Statistical significance was set at $P < 0.05$.

3. Results

3.1. General conditions

Among 20 female SD rats, 18 were successfully conceived, one of them had a miscarriage, and 17 of the pregnant rats eventually gave birth. There were 9 pregnant rats in the normal diet group and 8 in the low protein diet group, respectively. The total number of pups in the two groups was 117 and 103, respectively, and the average litter size per rat was (13.00 ± 1.66) and (12.88 ± 2.10) , the difference was not statistically significant ($F = 0.019$, $P = 0.893$). The average birth weight of the pups of the two groups was (7.05 ± 0.57) g and (5.77 ± 0.55) g, respectively, and the difference was statistically significant ($F = 289.309$, $P = 0.000$).

The mean birth weight minus two standard deviations (5.91g) was used as the criterion for IUGR pups in this experiment. Pups with birth weight lower than 5.91g in the normal diet group were excluded from the experiment, and 40 pups were randomly selected into the NBW group. Pups with birth weight lower than 5.91g in low-protein diet group were considered as IUGR pups, and 40 IUGR pups were randomly selected into IUGR group. The incidence of IUGR pups in low protein diet group was 70.87%, which was higher than that in normal diet group (4.27%), and the difference was statistically significant ($\chi^2 = 106.17$, $P = 0.000$), there was no significant difference in sex between the two groups ($\chi^2 = 0.029$, $P = 0.893$). (Table 3).

3.2. Birth weight and brain weight

IUGR pups exhibited a birth weight lower than the 10th percentile of birth weight for NBW pups (5.39 ± 0.44 g vs. 7.00 ± 0.26 g, $P < 0.001$). In addition, brain weight at birth was significantly lower in IUGR pups than in NBW pups (0.23 ± 0.02 g vs. 0.28 ± 0.02 g, $P < 0.001$). However, weight and brain weight did not significantly differ between IUGR and NBW pups on DOL 28 or 56. (Fig. 2A–F).

Table 3
General conditions.

Group	Pregnant rats		Total litter size		Litter size per rat		Birth weight of pups		IUGR in pups		Males in pups	
	n		n		$(\bar{x} \pm s, n)$	$(\bar{x} \pm s, g)$	n	%	n	%		
Normal diet	9		117		13.00 ± 1.66	7.05 ± 0.57	5	4.27	60	51.3		
Low-protein diet	8		103		12.88 ± 2.10	5.77 ± 0.55	73	70.87	54	52.4		
F/χ^2					0.019	289.309		106.170		0.029		
P					0.893	0.000		0.000		0.893		

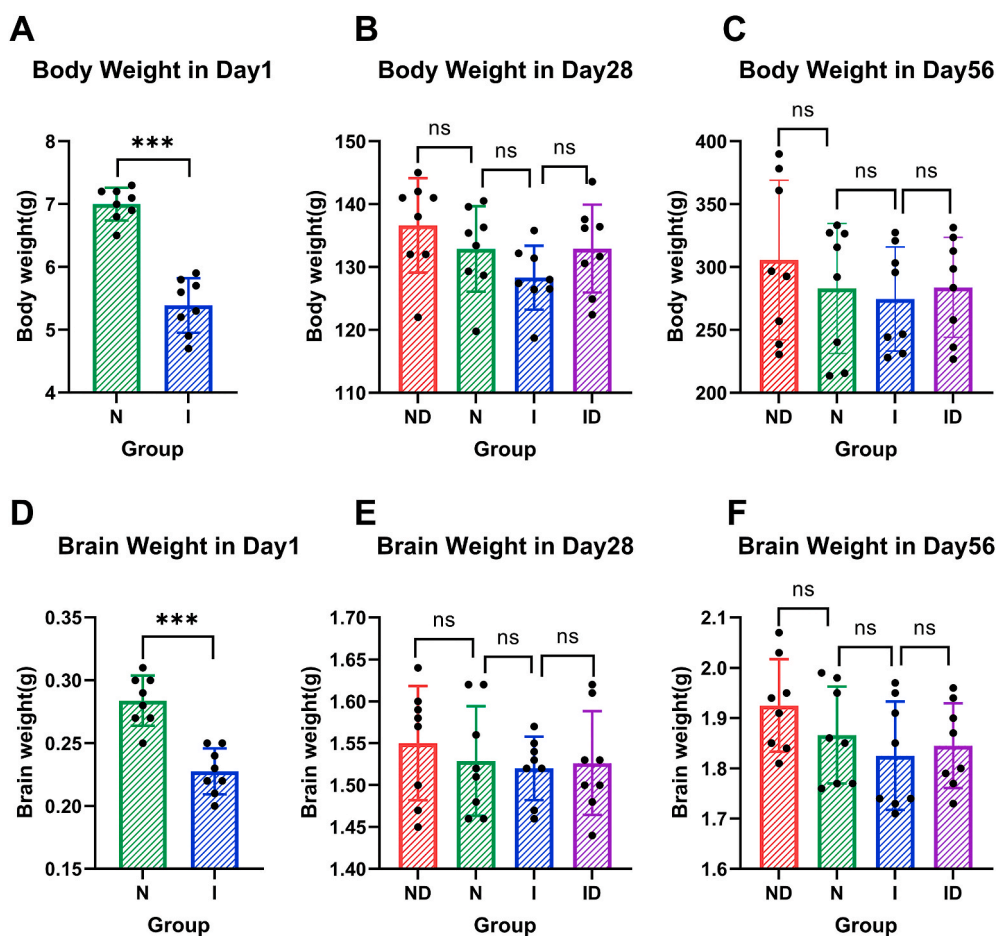


Fig. 2. Changes in body weight and brain weight in each groups over time.

3.3. Learning and memory function

The Morris water maze test was used to explore learning and memory function in IUGR offspring. On DOL 23–27, latency was longer in Group I than in Group N but shorter in group ID than in Group I. The differences between Group N and Group ND were not significant in terms of spatial navigation. The spatial probe test indicated that Group I crossed the target fewer times than Group N (1.38 ± 0.92 vs. 5.50 ± 3.12 , $P = 0.013$). In contrast, Group ID crossed the target more times than Group I (3.25 ± 1.39 vs. 1.38 ± 0.92 , $P = 0.045$), while there were no significant differences between Group N and Group ND (5.50 ± 3.12 vs. 5.00 ± 2.27 , $P = 1$) on DOL 28. On DOL 51–55, latency was longer in Group I than in Group N but shorter in group ID than in Group I. The differences between Group N and Group ND were not significant in terms of spatial navigation. The spatial probe test indicated that Group I crossed the target fewer times than Group N (1.00 ± 0.93 vs. 4.75 ± 2.76 , $P = 0.035$). In contrast, Group ID crossed the target more times than Group I (3.63 ± 1.30 vs. 1.00 ± 0.93 , $P = 0.003$), while there were no significant differences between Group N and Group ND (4.75 ± 2.76 vs. 3.63 ± 1.30 , $P = 0.975$) on DOL 56. (Fig. 3A–F).

3.4. Pathological changes of the hippocampus

Hematoxylin and eosin staining revealed that IUGR offspring exhibited sparse hippocampal neurons, irregular arrangement, and uneven cell size. However, DHA intervention attenuated the loss of hippocampal neurons. (Fig. 4A–T).

3.5. Ultrastructural changes of the hippocampal neurons

Electron microscopy revealed changes in the ultrastructure of hippocampal neurons in IUGR offspring. The nuclear chromatin was condensed, the perinuclear space was narrowed, the mitochondria were swollen, the cell membrane was damaged, and the cell contents had been released. However, DHA intervention attenuated these changes. (Fig. 5A–T).

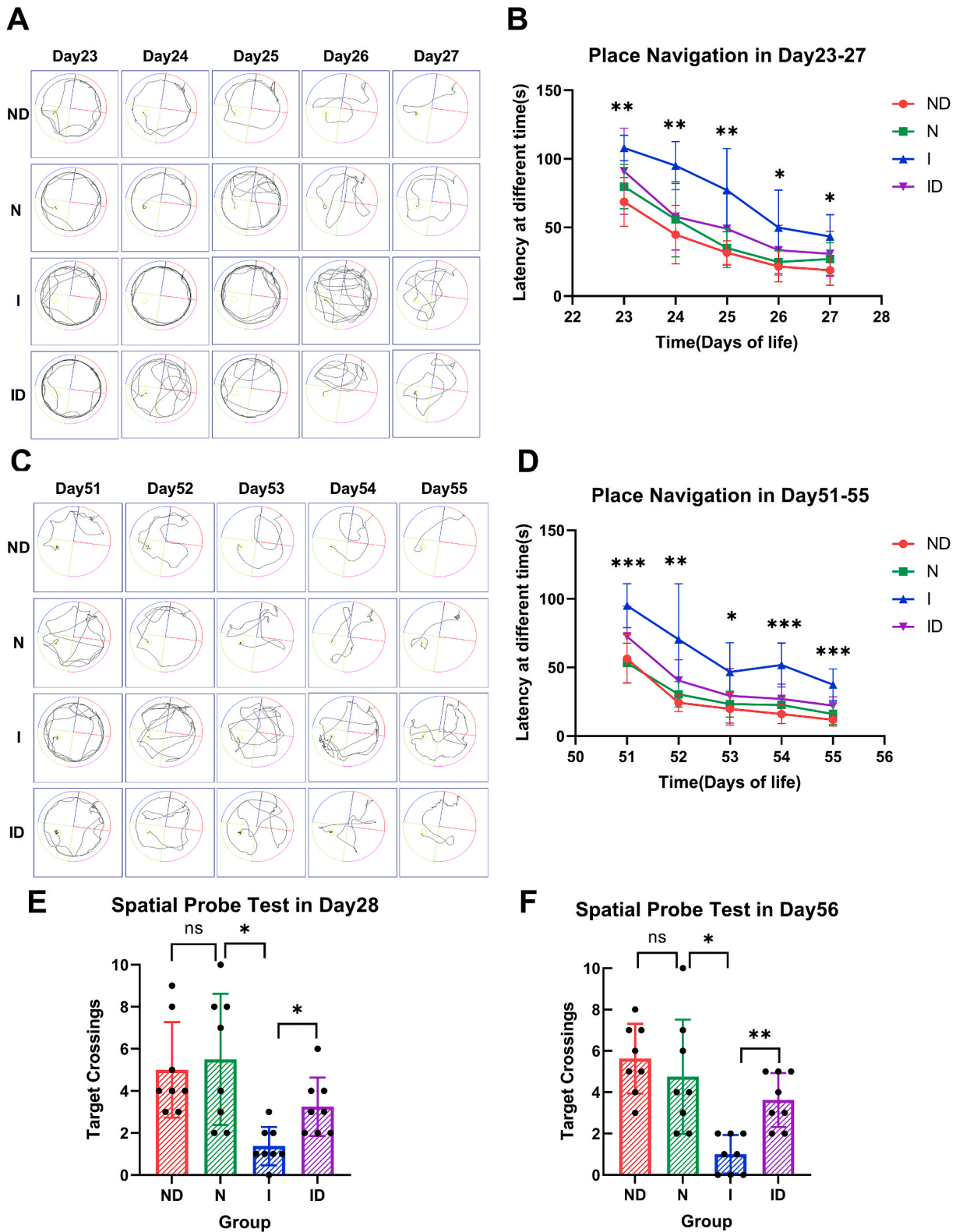


Fig. 3. Learning and memory function based on performance in the Morris water maze test.

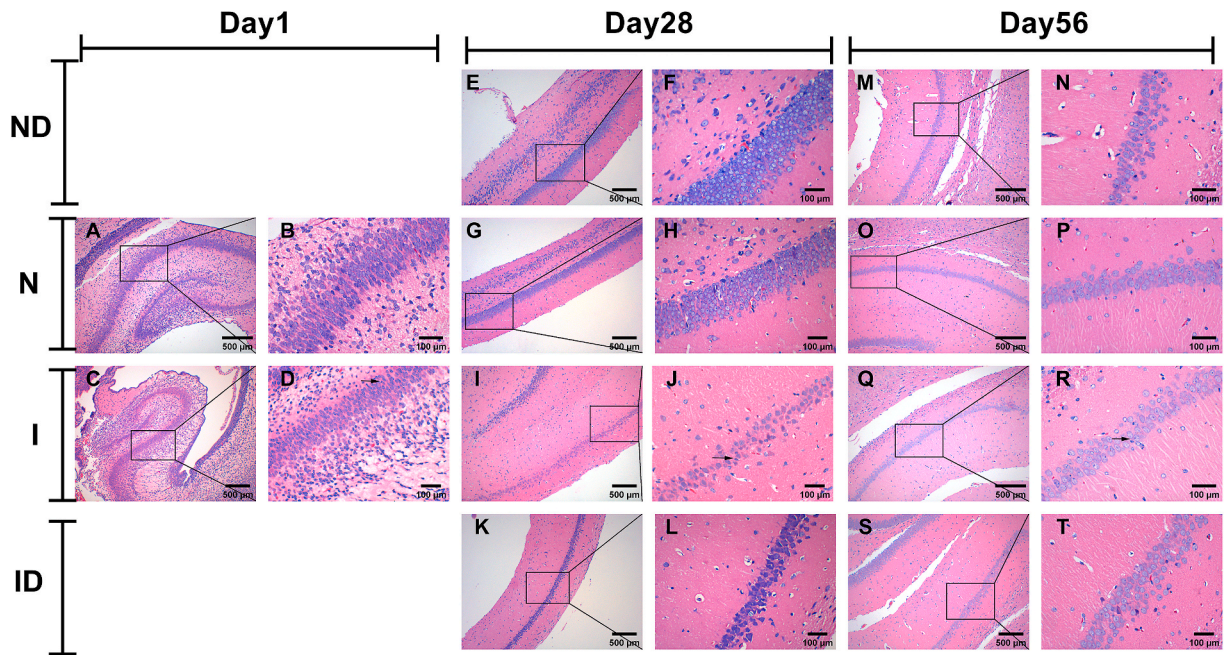


Fig. 4. Morphological structure of the hippocampus based on hematoxylin and eosin staining. The highlighted hippocampal subregions regions is CA1. The arrows show that hippocampal neurons are pyknotic, sparse, irregularly arranged.

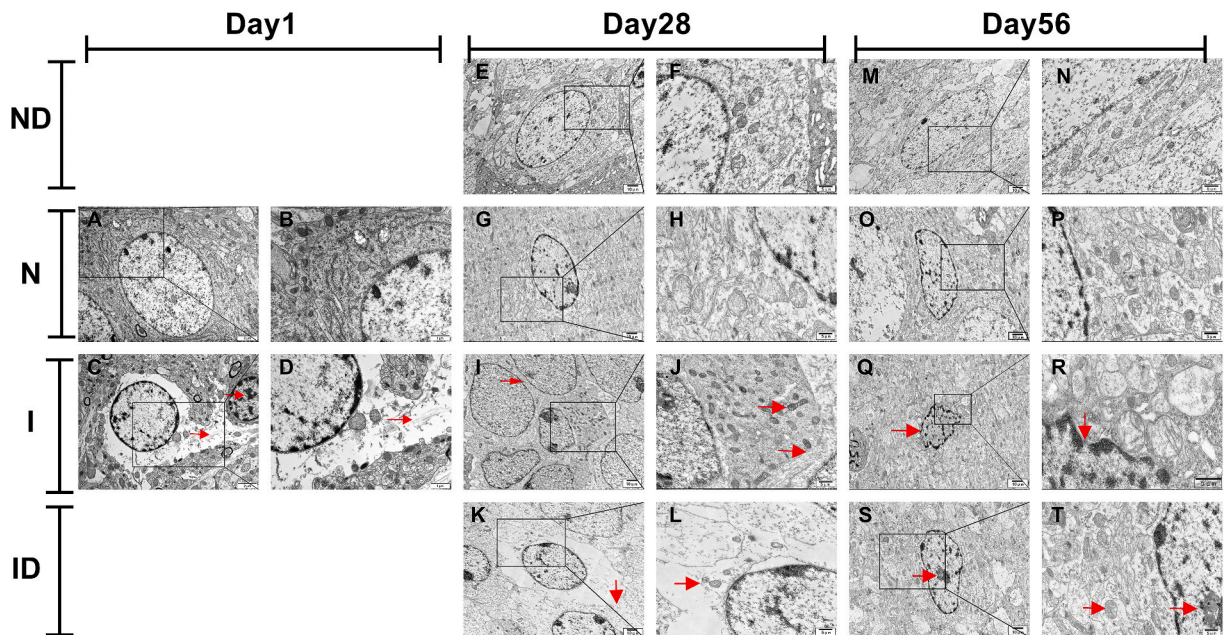


Fig. 5. Ultrastructure of hippocampal neurons as observed via electron microscopy. The arrows in figure C show the damaged cell membrane and condensed nuclear chromatin. The arrow in figure D shows the damaged cell membrane. The arrow in figure I shows the perinuclear space was narrowed. The arrows in figure J show the mitochondria were swollen and cell membrane was damaged. The arrow in figure K shows the damaged cell membrane. The arrow in figure L shows the cell membrane was damaged and the cell contents had been released. The arrows in figure Q, R, S show the condensed nuclear chromatin. The arrows in figure T show the swollen mitochondria and condensed nuclear chromatin.

3.6. The GSDMD immunofluorescence staining of the hippocampus

Positive GSDMD staining was significantly higher in Group I than in Group N on DOL 1, 28 and 56. In contrast, this value was significantly lower in Group ID than in Group I on DOL 28 and 56, and there were no significant differences between Groups ND and N.

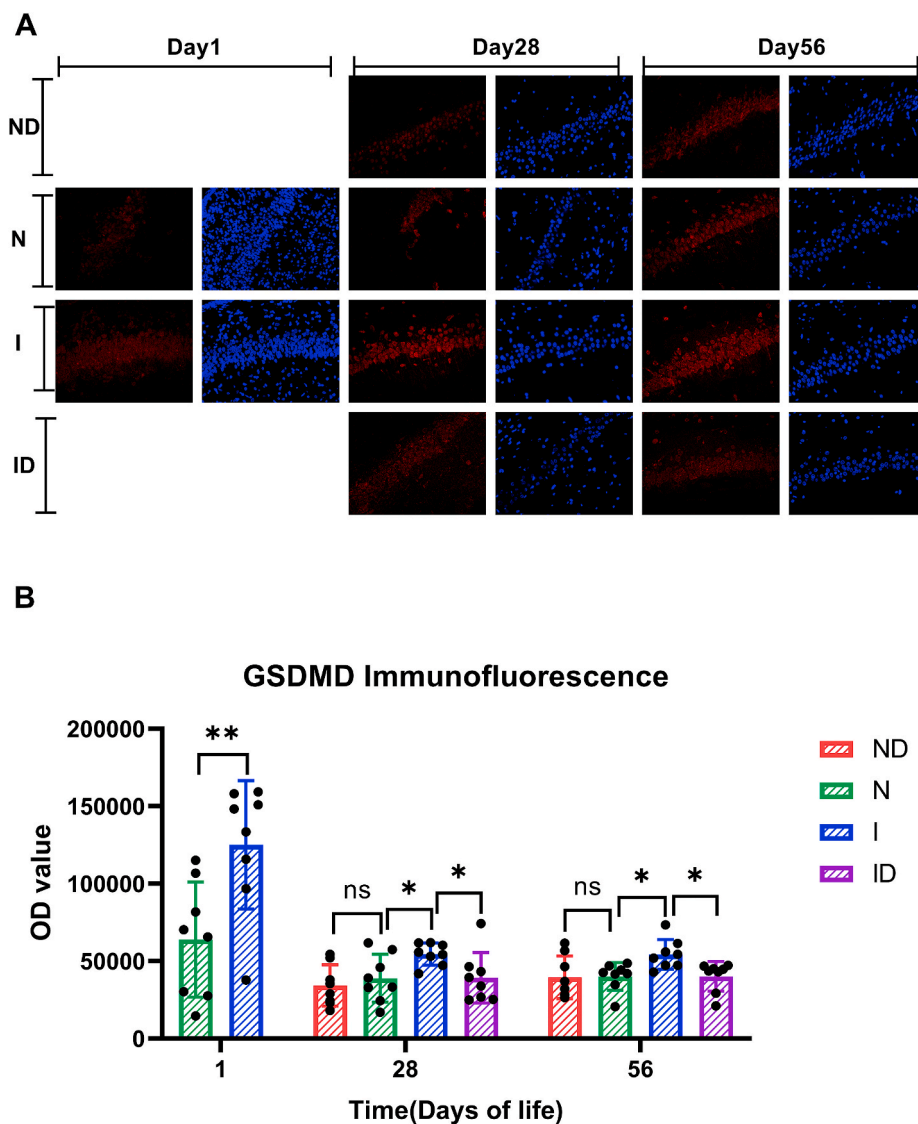


Fig. 6. GSDMD immunofluorescence staining.

(Fig. 6A–B).

3.7. The mRNA expression of *NLRP1*, *caspase-1*, and *GSDMD* in the hippocampus

The RT-qPCR analysis revealed that the relative mRNA levels of *NLRP1*, *caspase-1*, and *GSDMD* were significantly higher in Group I than in Group N on DOL 1, 28, and 56. At the same time, they were significantly lower in Group ID than in Group I on DOL 28 and 56. There were no significant differences between groups ND and N on DOL 28 or 56. (Fig. 7A–I).

3.8. The protein expression of *NLRP1*, *procaspase-1*, *cleaved caspase-1*, and *GSDMD-N* in the hippocampus

WB analysis revealed that the relative protein levels of *NLRP1*, *procaspase-1*, *cleaved caspase-1*, and *GSDMD-N* were significantly higher in Group I than in Group N on DOL 1, 28, and 56. At the same time, there were no significant differences between Groups ND and N on DOL 28 or 56. Protein expression of *NLRP1*, *procaspase-1*, and *cleaved caspase-1* was significantly lower in Group ID than in Group I on DOL 28 and 56. While *GSDMD-N* was significantly lower in Group ID than in Group I on DOL 56, there was no significant difference on DOL 28. (Fig. 8A–F).

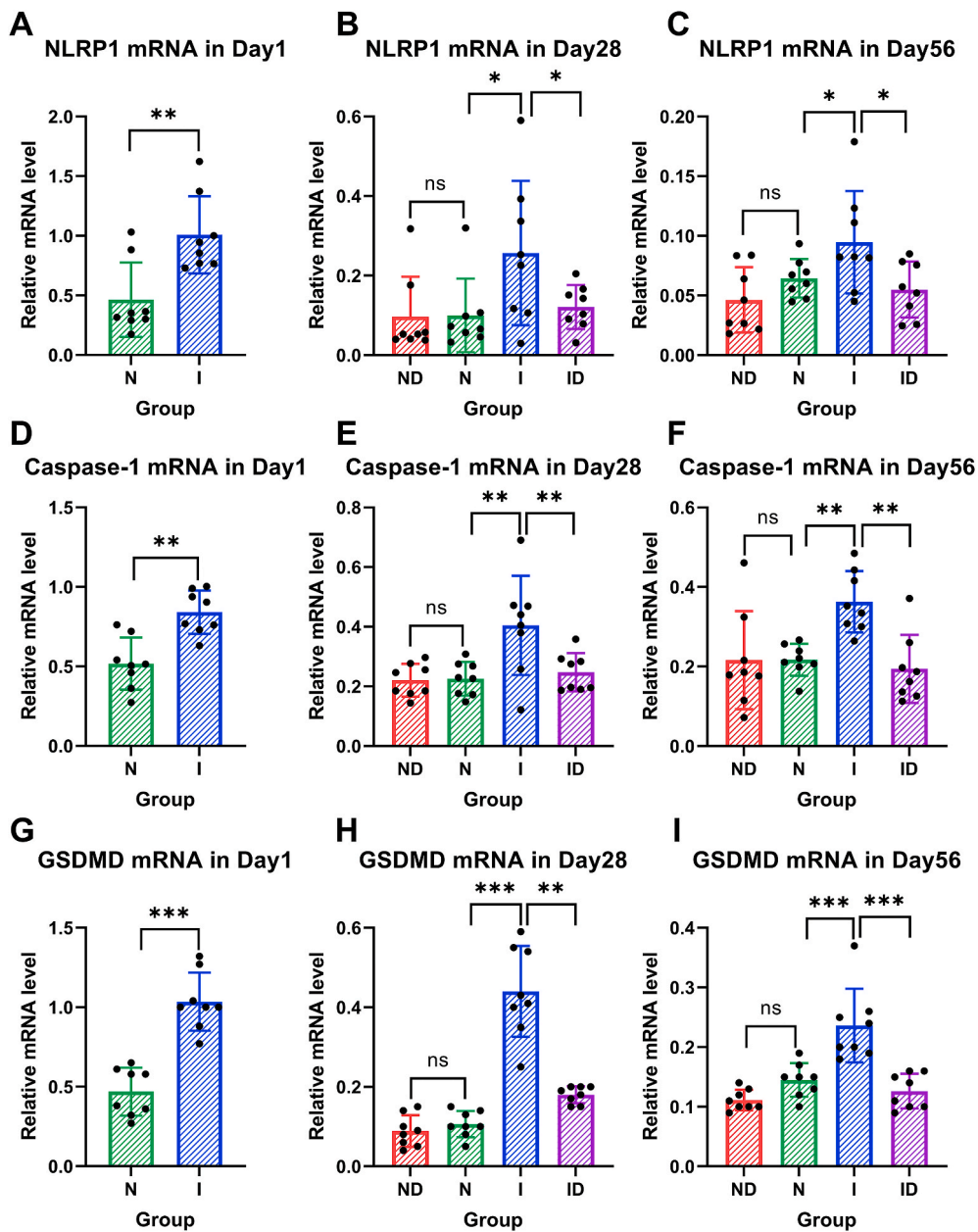


Fig. 7. The mRNA expression of nuclear localization leucine-rich-repeat protein 1 (NLRP1), caspase-1, and GSDMD in the hippocampus as detected using quantitative reverse transcription PCR (RT-qPCR).

3.9. The quantification of IL-1 β and IL-18 in the hippocampus

ELISA was used to examine the release of the inflammatory cytokines IL-1 β and IL-18 in the hippocampus. IL-1 β and IL-18 levels were higher in Group I than in Group N on DOL 1, 28, and 56. Levels of IL-1 β and IL-18 were lower in Group ID than in Group I, and there was no significant difference between Groups N and ND on DOL 28 or 56. (Fig. 9A–F).

4. Discussion

4.1. The model of IUGR offspring was successfully established by low protein diet throughout pregnancy

The normal development of fetus is affected by the interaction between mother, placenta and fetus and the stable environment which them form. Malnutrition during pregnancy and placental insufficiency are common causes of IUGR [3]. IUGR model preparation

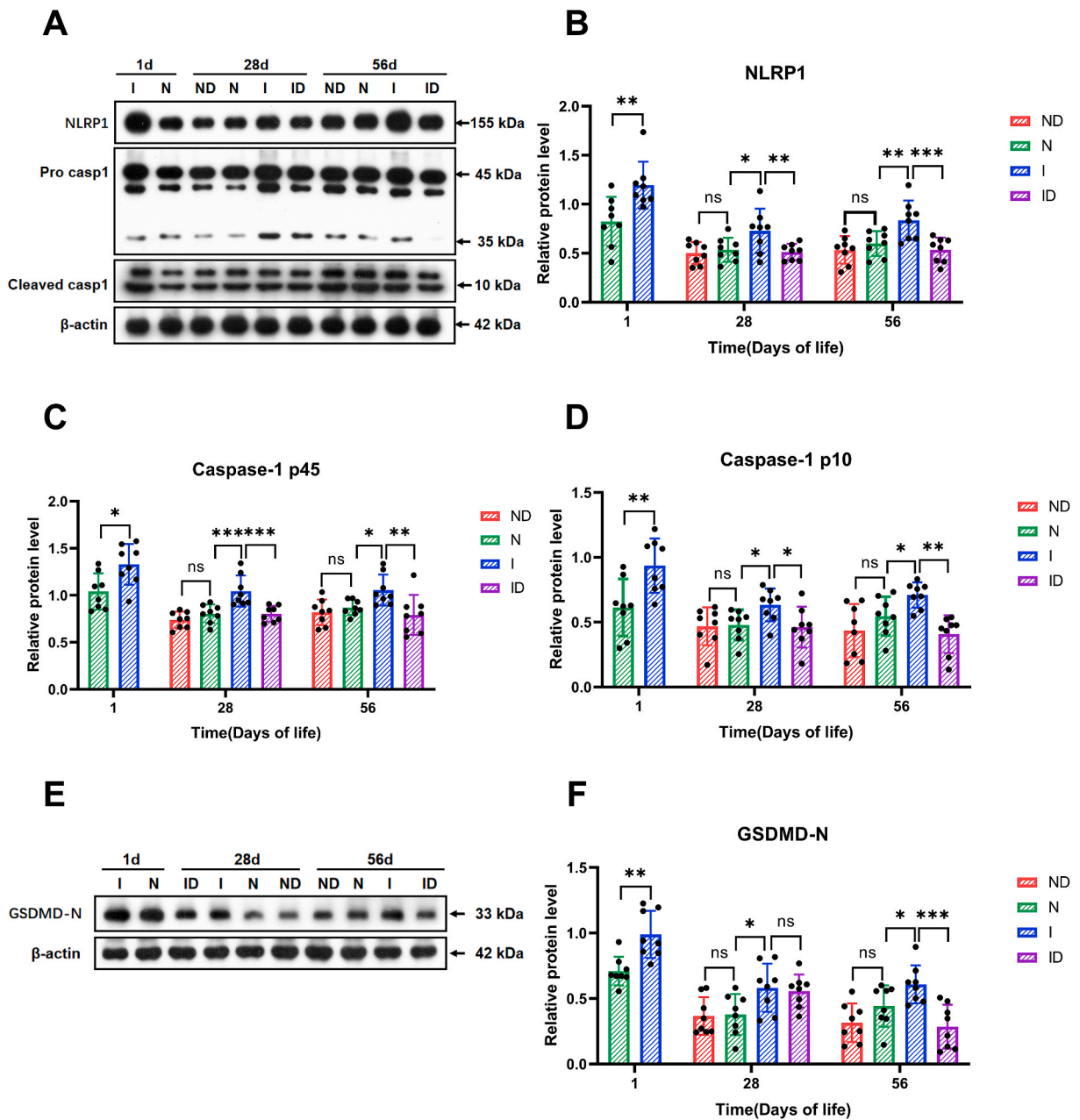


Fig. 8. Protein expression of NLRP1, procaspase-1, cleaved caspase-1, and active gasdermin-D (GSDMD-N) in the hippocampus as detected by Western blotting. Full, non-adjusted images of Fig. 8(A,E) see the supplementary material.

methods include low-protein diet, uterine artery ligation, hypoxia inhalation, anti-metabolic drugs (e.g., reliquicin method), passive smoking method and platelet activating factor method. Low-protein diet and uterine artery ligation are the two most widely used methods for preparation of IUGR model [22]. After ligation of uterine arteries, the blood supply of placenta is reduced, and the transportation of nutrients is obstructed, resulting in restriction of fetal growth and development. The early method was completed ligation of bilateral uterine arteries, with high stillbirth rate and low incidence of IUGR. After improvement, partial uterine artery ligation was adopted. Although the above shortcomings were improved, the operation was difficult to operate, too tight ligation of uterine artery was associated with increased stillbirth rate, and too loose ligation of uterine artery was associated with reduced incidence of IUGR [22]. The low-protein diet is used to prepare the IUGR model by reducing the nutrition supply of the fetus through the low-protein diet on the premise of ensuring the same total energy, thus affecting its growth and development. This method has advantages of simple operation, higher rate of success and lower rate of stillbirth [23]. Construction of the IUGR model using this method is more in line with the principle underlying the occurrence of IUGR in developing countries (i.e., nutritional reasons). In the

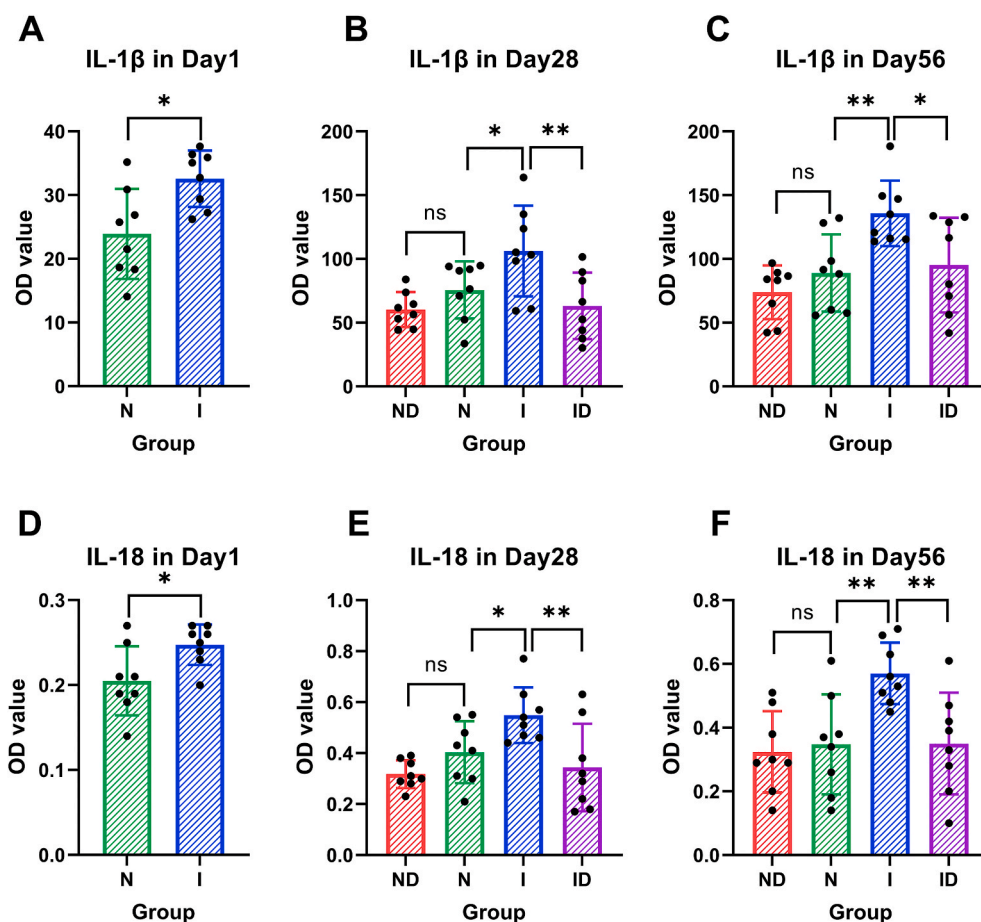


Fig. 9. Quantification of inflammatory cytokines interleukin (IL)-1 β and IL-18 in the hippocampus as detected via enzyme-linked immunosorbent assay (ELISA).

present study, we successfully established a model of IUGR by feeding pregnant rats with a 10% low-protein diet, consistent with the results of previous study [7].

4.2. Cognitive impairment of IUGR pups persisted into adulthood, and DHA attenuated this impairment

Our study suggested the birth weight and brain weight of IUGR pups were significantly lower than those of NBW pups, indicating that IUGR not only affected the development of body, but also affected the development of brain. This may be due to IUGR deprives the oxygen and nutrients needed for brain [24], thereby affecting the normal development of brain and causing damage to CNS. However, there were no significant differences in body weight and brain weight between IUGR and NBW pups on DOL 28 and 56, indicating that IUGR pups had completed the catch-up growth in body and brain development on DOL 28.

Analysis of Morris water maze test results revealed that IUGR pups exhibited impairments in learning and memory function, which persisted into adulthood. IUGR can cause different degrees of damage on the CNS in infants and young children, but the effects in adulthood are controversial. Some animal studies had shown that IUGR pups had decreased spatial learning and memory abilities and persisted into adulthood [25], which is consistent with the results of our study. However, some studies had found that IUGR had no effect on cognitive function in adult [26], which may be due to the existence of neurorepair mechanisms during brain development and the role of catch-up growth.

Llanos et al. found that the formation of DHA was reduced in IUGR neonatal, and the restriction of docosaentaenoic acid converting to DHA may be the main reason for the abnormal DHA metabolism in IUGR children [27]. However, there was few study on whether DHA supplementation can improve the cognitive impairment of IUGR. In our study, DHA supplementation from DOL 1 improved the cognitive impairment of IUGR offspring in childhood and adulthood.

4.3. Pathological changes in the hippocampus and ultrastructural changes in the hippocampal neurons

HE staining in our study revealed pathological changes in the hippocampus, consistent with the results of other studies [3,28].

However, the present study is the first to report ultrastructural changes in hippocampal neurons in IUGR pups based on electron microscopy findings. Our electron microscopy analysis revealed that IUGR offspring exhibited nuclear chromatin pyknosis in hippocampal neurons, which is also observed during apoptosis. However, cell swelling, cell membrane rupture, and release of cell contents were also observed, consistent with the morphological characteristics of pyroptosis.

4.4. Pyroptosis of hippocampal neurons in IUGR offspring and the effect of DHA

The two conditions necessary for promoting pyroptosis are the activation of inflammasomes and the splicing and maturation of the pro-inflammatory factors IL-1 β and IL-18 [29]. The roles of the NLRP1 and NLRP3 inflammasomes in the nervous system have been studied extensively. NLRP3 inflammasomes mainly exist in microglia and play a more important role in inflammatory cytokine secretion and subsequent inflammatory events. In contrast, NLRP1 inflammasomes are mainly found in neurons and play a more important role in pyroptosis [30]. The canonical pyroptosis pathway is mediated by the activation of caspase-1, while GSDMD is the executive protein involved in pyroptosis [31]. Given that we observed increased expression of GSDMD in hippocampal neurons, increased mRNA and protein expression of NLRP1, caspase-1, and GSDMD, and increased quantification of IL-1 β and IL-18 in hippocampus, the present results suggest that IUGR leads to pyroptosis of hippocampal neurons, which can last until DOL 56. However, error bars of DOL 28 and 56 rats were much smaller compared to the DOL 1, it may be related to catch-up growth, thus the differences between individuals decrease with the increase of age. This study is the first to report pyroptosis as a mechanism underlying cognitive impairment in IUGR offspring.

Importantly, the present results indicate that DHA intervention in the early postnatal period reduced the immunofluorescence expression of GSDMD in hippocampal neurons, reduced the mRNA expression of NLRP1, caspase-1, GSDMD, the protein expression of NLRP1, caspase-1, GSDMD-N, and the quantification of IL-1 β and IL-18 in the hippocampus of IUGR offspring. These results suggest that the anti-inflammatory effects of DHA may be related to its ability to attenuate pyroptosis and NLRP1 inflammasome activation, thus alleviating brain injury. Previous studies on the anti-inflammatory mechanism of DHA mostly focused on reducing activation of the NLRP3 inflammasome. Only one study by Chen et al. has reported that DHA can reduce the activation of the NLRP1 inflammasome in placental trophoblasts [19]. Our study is the first to demonstrate that DHA reduces activation of the NLRP1 inflammasome in the hippocampus.

However, this study has its limitations. First, the preparation of animal models is more likely to be related to nutrition during pregnancy. Therefore, the mechanism of IUGR in relation to the placenta cannot be fully reflected. In addition, this study did not examine the active targets of DHA in vitro and in vivo (e.g., inhibiting a target of the pyroptosis pathway and then conducting a DHA intervention to observe the different effects of DHA).

5. Conclusion

Our findings support the notion that cognitive impairment can persist until adulthood in IUGR offspring and that such impairment may be related to pyroptosis of hippocampal neurons. Early intervention with DHA may help to attenuate cognitive impairment and reduce pyroptosis of hippocampal neurons in IUGR offspring. Further research should investigate the upstream pathways and regulatory targets of pyroptosis related to cognitive impairment in IUGR.

Author contribution statement

Lijia Wan: Conceived and designed the experiments; Performed the experiments; Analyzed and interpreted the data; Wrote the paper.

Xiaori He, Mingfeng He: Contributed reagents, materials, analysis tools or data.

Yuanqiang Yu, Weiming Jiang; Can Liang: Performed the experiments.

Kaiju Luo, Xiaoyun Gong, Yonghui Yang; Qingyi Dong: Analyzed and interpreted the data.

Pingyang Chen: Conceived and designed the experiments; Contributed reagents, materials, analysis tools or data; Wrote the paper.

Funding statement

Prof. Pingyang Chen was supported by Hunan Provincial Natural Science Foundation General Project [2020JJ4781].

Mingfeng He was supported by Youth Foundation of National Natural Science Foundation of China [81801508].

Data availability statement

Data included in article/supp. material/referenced in article.

Declaration of interest's statement

The authors declare no competing interests.

Acknowledgments

None.

Appendix A. Supplementary data

Supplementary data related to this article can be found at <https://doi.org/10.1016/j.heliyon.2023.e12920>.

References

- [1] D. Sharma, et al., Intrauterine growth restriction - part 1, *J. Matern. Fetal Neonatal Med.* 29 (24) (2016) 3977–3987.
- [2] C. Sacchi, et al., Association of intrauterine growth restriction and small for gestational age status with childhood cognitive outcomes: a systematic review and meta-analysis, *JAMA Pediatr.* 174 (8) (2020) 772–781.
- [3] J. Chen, et al., Cognitive and behavioral outcomes of intrauterine growth restriction school-age children, *Pediatrics* 137 (4) (2016).
- [4] C. Gilchrist, et al., Intrauterine growth restriction and development of the hippocampus: implications for learning and memory in children and adolescents, *Lancet Child Adolesc Health* 2 (10) (2018) 755–764.
- [5] B. Fleiss, et al., Knowledge gaps and emerging research areas in intrauterine growth restriction-associated brain injury, *Front. Endocrinol.* 10 (2019) 188.
- [6] L. Wan, K. Luo, P. Chen, Mechanisms underlying neurologic injury in intrauterine growth restriction, *J. Child Neurol.* 36 (9) (2021) 776–784.
- [7] J. Chen, et al., miR-199a-5p regulates sirtuin1 and PI3K in the rat hippocampus with intrauterine growth restriction, *Sci. Rep.* 8 (1) (2018), 13813.
- [8] H. Kim, et al., AIM2 inflammasome contributes to brain injury and chronic post-stroke cognitive impairment in mice, *Brain Behav. Immun.* 87 (2020) 765–776.
- [9] L. Poh, et al., AIM2 inflammasome mediates hallmark neuropathological alterations and cognitive impairment in a mouse model of vascular dementia, *Mol. Psychiatr.* 26 (8) (2021) 4544–4560.
- [10] X.E. Xu, et al., Caspase-1 inhibitor exerts brain-protective effects against sepsis-associated encephalopathy and cognitive impairments in a mouse model of sepsis, *Brain Behav. Immun.* 80 (2019) 859–870.
- [11] Y. Hu, et al., Pyroptosis, and its role in central nervous system disease, *J. Mol. Biol.* 434 (4) (2022), 167379.
- [12] F. Shao, K.A. Fitzgerald, Molecular mechanisms and functions of pyroptosis, *J. Mol. Biol.* 434 (4) (2022), 167461.
- [13] T.L. Thurston, et al., Growth inhibition of cytosolic Salmonella by caspase-1 and caspase-11 precedes host cell death, *Nat. Commun.* 7 (2016), 13292.
- [14] J. Amin, D. Boche, S. Rakic, What do we know about the inflammasome in humans? *Brain Pathol.* 27 (2) (2017) 192–204.
- [15] J.D. Lunemann, et al., Targeting inflammasomes to treat neurological diseases, *Ann. Neurol.* 90 (2) (2021) 177–188.
- [16] E. Talamonti, et al., Impairment of DHA synthesis alters the expression of neuronal plasticity markers and the brain inflammatory status in mice, *Faseb. J.* 34 (2020) 2024–2040.
- [17] T. Inoue, et al., Omega-3 polyunsaturated fatty acids suppress the inflammatory responses of lipopolysaccharide-stimulated mouse microglia by activating SIRT1 pathways, *Biochim. Biophys. Acta Mol. Cell Biol. Lipids* 1862 (5) (2017) 552–560.
- [18] C. Lin, et al., Omega-3 fatty acids regulate NLRP3 inflammasome activation and prevent behavior deficits after traumatic brain injury, *Exp. Neurol.* 290 (2017) 115–122.
- [19] C.Y. Chen, et al., Omega-3 polyunsaturated fatty acids reduce preterm labor by inhibiting trophoblast cathepsin S and inflammasome activation, *Clin. Sci. (Lond.)* 132 (20) (2018) 2221–2239.
- [20] Q. Wang, et al., Different concentrations of docosahexanoic acid supplement during lactation result in different outcomes in preterm Sprague-Dawley rats, *Brain Res.* 1678 (2018) 367–373.
- [21] C.D. Barnhart, D. Yang, P.J. Lein, Using the Morris water maze to assess spatial learning and memory in weanling mice, *PLoS One* 10 (4) (2015) e0124521.
- [22] D.S. Hunter, et al., Programming the brain: common outcomes and gaps in knowledge from animal studies of IUGR, *Physiol. Behav.* 164 (Pt) (2016) 233–248.
- [23] V. Zohdi, et al., Developmental programming of cardiovascular disease following intrauterine growth restriction: findings utilising a rat model of maternal protein restriction, *Nutrients* 7 (1) (2014) 119–152.
- [24] M. Dubovicky, Neurobehavioral manifestations of developmental impairment of the brain, *Interdiscipl. Toxicol.* 3 (2) (2010) 59–67.
- [25] Y. Zhang, N. Li, Z. Yang, Perinatal food restriction impaired spatial learning and memory behavior and decreased the density of nitric oxide synthase neurons in the hippocampus of adult male rat offspring, *Toxicol. Lett.* 193 (2) (2010) 167–172.
- [26] R.B. Jensen, et al., Cognitive ability in adolescents born small for gestational age: associations with fetal growth velocity, head circumference and postnatal growth, *Early Hum. Dev.* 91 (12) (2015) 755–760.
- [27] A. Llanos, et al., Infants with intrauterine growth restriction have impaired formation of docosahexanoic acid in early neonatal life: a stable isotope study, *Pediatr. Res.* 58 (4) (2005) 735–740.
- [28] F.C. Duran, et al., Influence of catch up growth on spatial learning and memory in a mouse model of intrauterine growth restriction, *PLoS One* 12 (5) (2017) e0177468.
- [29] V.A. Rathinam, K.A. Fitzgerald, Inflammasome complexes: emerging mechanisms and effector functions, *Cell* 165 (4) (2016) 792–800.
- [30] S. Kesavardhana, T.D. Kanneganti, Mechanisms governing inflammasome activation, assembly and pyroptosis induction, *Int. Immunol.* 29 (5) (2017) 201–210.
- [31] J. Shi, et al., Cleavage of GSDMD by inflammatory caspases determines pyroptotic cell death, *Nature* 526 (7575) (2015) 660–665.